Received: 28 July 2022 | Revised: 27 September 2022 | Accepted: 5 November 2022

IET Generation, Transmission & Distribution

DOI: 10.1049/gtd2.12680

The Institution of Engineering and Technology WILEY

ORIGINAL RESEARCH

Very fast transient overvoltage calculation and evaluation for 500-kV gas insulated substation power substation with double circuit and long gas insulated substation busbar

Runyu Fu | **Jianguo Wang** | **Jianping Wang** | **Mi Zhou** | **Cai Li** | **Yating Zhao** | **Yadong Fan**

School of Electrical Engineering and Automation, Wuhan University, Wuhan, China

Correspondence
Jianguo Wang and Jianping Wang, School of Electrical Engineering and Automation, Wuhan University, Wuhan, China.
Email: wjg@whu.edu.cn;

Abstract
The operation of disconnectors in gas insulated substation (GIS) or power plant will produce very fast transient overvoltage (VFTO), which is considered to have serious harm to transformer longitudinal insulation and other high-voltage equipment insulation. VFTO may also lead to secondary circuit failure. In this paper, the holistic modelling of 500 kV GIS step-up substation equipment with a double circuit and long GIS busbar in a coastal power plant is established using Electromagnetic Transient Program (EMTP). The authors calculated the VFTO waveform that may be generated in different operations of the GIS substation. The authors analyze the amplitude and frequency characteristics of the VFTO waveform at lightning arresters and the entrance of transformers and find that the amplitude of VFTO at the entrance of #1 MT is less than its impulse withstand voltage. In some cases, the VFTO waveform at the entrance of #1 MT has high-frequency content with fast attenuation. The VFTO waveform generated when operating the disconnector close to the arrester will cause the arrester to act many times and count frequently in a short time.

1 | INTRODUCTION

Gas-insulated switchgear is widely used in power systems because of its compact structure and high reliability. The switching operation of disconnectors in GIS systems may lead to very fast transient overvoltage (VFTO) [1, 2] with extremely high-frequency oscillation. The disconnector operates slowly, and arc reburning occurs repeatedly during operation, resulting in multiple VFTOs. Due to their frequent occurrence, it will lead to the ageing of system insulation [3, 4]. In addition to causing faults in the gas-insulated bus duct of the substation, VFTO may also lead to the faults in protection and control circuit [5]. The insulation fault of GIS caused by VFTO has attracted the attention of researchers and becomes a research hotspot all over the world [6–8].

Experimental research on VFTO characteristics has been carried out, in which the amplitude, frequency, waveform and other characteristics are the focus of experimental research. The main VFTO simulation method is based on circuit model, and the most common method is to establish simulation models for GIS components by using the electromagnetic transient simulation program such as electromagnetic transient program (EMTP). In addition, the method of three-dimensional electromagnetic field simulation can also be used to study by solving the Maxwell equation of the three-dimensional structure of the actual GIS [9, 10].

The magnitude of VFTO amplitude is mainly determined by the breakdown voltage between the fixed contact and the moving contact [8]. The VFTO amplitude range measured in the in-service substation is usually 1.5 p.u. to 2.5 p.u. [2, 11–13], frequency range is 100 kHz to 40 MHz [14, 15]. With the propagation of travelling waves on the GIS busbar, the high-frequency components of VFTO were reduced, while the lower frequency components lasted longer relatively [4, 16].

Compared with experimental research, simulation calculation has the advantages of easy implementation and convenient expansion. It is an important method to study VFTO [17, 18]. Most previous publications assumed that the initial trap charge was 1 p.u. [19]. However, Boggs and Chu et al. [1] have carried out field tests, and their measurement results indicate that transients do not exceed 2 p.u. at the point of measurement, and the trapped charge left on the load side is less than 0.3 p.u. The trapped charge on the load side of the disconnector decays so slowly that it can be considered to be constant for the period of interest [11]. The peak value of VFTO calculated by simulation may reach 3 p.u. [5, 7], and the frequency of VFTO is usually 100 kHz to 100 MHz [17, 20, 21].

The step-up substation of the 500 kV GIS power plant in this paper is located near the sea, with serious salt fog, and the pollution level of the surrounding environment is ‘very heavy’ according to the standard of classification. After the #1 main transformer is put into operation, there is no abnormal state within 3 years. The H and J outgoing lines of 500 kV substation trip 100 times in 3 years. After phase B grounding fault of primary H transmission line and J transmission line, it was found that #1 transformer shell and winding were deformed. The #1 arrester counter does not count, and the voltage transformer of transformer is damaged after the accident.

In this paper, we establish a simulation model of the whole 500-kV step-up substation of a power plant with long GIS busbar. The VFTO waveforms that may be generated during several operation modes are calculated.

In Section 2, we introduce the simulation model and calculation condition. Section 3 presents the calculation result under different work conditions. Section 4 presents the analysis and discussion of the calculation result. The conclusion is presented in the last section.

2 | SIMULATION MODEL AND CALCULATION CONDITIONS

2.1 | Substation main wiring structure

We built the B-phase wiring model of the whole substation. The single-line diagram of the 500-kV GIS substation is shown in Figure 1.

The simulated power plant has two 660 MVA generator sets. The two sets are connected to the 500-kV power distribution device in the plant by generator transformer unit wiring. The 500-kV high-voltage side adopts 3/2 connection mode, with a total of two outgoing lines, of which the outgoing line on the left is the J line and on the right is the H line. #1MT and #2 MT are main transformers, and #3 MT is stand-by transformers. #3 MT was not put into operation on that fault day, and the circuit breaker and disconnector between 3 MT and the busbar were disconnected. #1LA and #2 LA are arresters for the transformer. HLA and JLA are arresters at the entrance of transmission lines. There is a 200-m-long GIS busbar between #1 VT and #1 LA and between #2 VT and #2 LA.

2.2 | Simulation models and parameter

We use ATP-EMTP electromagnetic transient calculation program to simulate the VFTO overvoltage of the 500-kV GIS substation.

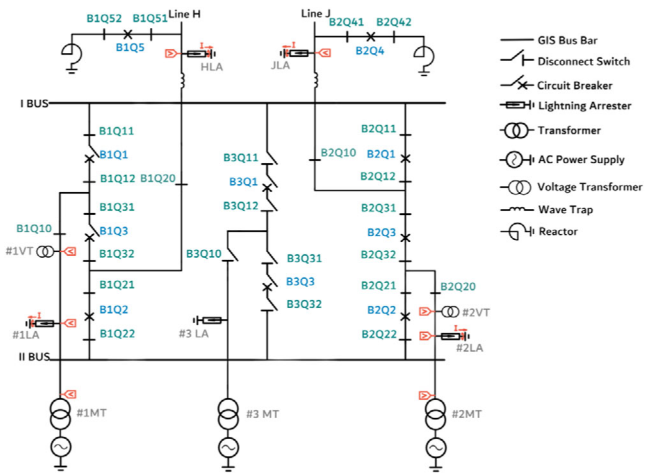

FIGURE 1 Main wiring diagram of simulated substation. The red mark in the figure is the voltage and current measurement point.

TABLE 1 Volt-ampere characteristics of lightning arrester

	Current (A)	0.001	100	1000	5000	10,000
HLA/JLA	Voltage (kV)	565	861.5	937.3	994.2	1019.8
#1LA/#2LA	Voltage (kV)	549	853.7	932.5	991.9	1018.6

The parallel form of equivalent inlet capacitance and equivalent impedance at the high voltage side is used to simulate the transformer.

The lightning arrester is simulated by a parallel connection of stray capacitance and non-linear resistance. The volt-ampere characteristic of non-linear resistance is determined according to the volt-ampere characteristic curve of the arrester, and its data are shown in Table 1.

GIS busbar, overhead transmission line and closed disconnector and circuit breaker are simulated by the equivalent lossless uniform transmission line. The disconnected circuit breaker and disconnector are simulated by equivalent fracture capacitance. The arc resistance is simulated by time-varying resistance, and its expression is

$$R(t) = R_0 e^{-\frac{t}{T_1}} + R_S e^{\frac{t}{T_2}} \ (\Omega) \tag{1}$$

where R_0 is 10^{12} Ω, R_S is 0.5 Ω, T_1 is 1 ns and T_2 is 1 μs.

2.3 | Simulation conditions

Considering the actual operation mode of the substation, the calculation conditions include H line outage operation, I bus outage operation and #1 MT outage operation under the working mode of two transformers with two outgoing lines, and working mode of #1 MT with H line outage operation, as shown in Table 2. During the opening process of the disconnector, we calculate the VFTO generated by arc reburning when the power supply voltage reaches the peak value under each working condition, and consider that the voltage caused by the

TABLE 2 Summary of simulation conditions

Working condition	Operation	Operation sequence	Operating equipment	Opened equipment (Except B3Q3, B3Q1, B3Q31, B3Q32, B3Q11, B3Q12)	Closed equipment	Trapped charge
Two transformers with two outgoing lines	H line outage operation	1	B1Q20	B1Q3, B1Q2, B1Q5	The other circuit breakers and disconnectors	−1.0 p.u./ −0.3 p.u.
		2	B1Q32	B1Q3, B1Q2, B1Q5, B1Q20	The other circuit breakers and disconnectors	−1.0 p.u./ −0.3 p.u.
		3	B1Q21	B1Q3, B1Q2, B1Q5, B1Q20, B1Q32	The other circuit breakers and disconnectors	−1.0 p.u./ −0.3 p.u.
	I-bus outage operation	4	B1Q11	B1Q1, B2Q1	The other circuit breakers and disconnectors	−1.0 p.u./ −0.3 p.u.
		5	B2Q11	B1Q1, B2Q1, B1Q11	The other circuit breakers and disconnectors	−1.0 p.u./ −0.3 p.u.
	#1 transformer outage operation	6	B1Q10	B1Q3, B1Q1	The other circuit breakers and disconnectors	−1.0 p.u./ −0.3 p.u.
		7	B1Q31	B1Q3, B1Q1, B1Q10	The other circuit breakers and disconnectors	−1.0 p.u./ −0.3 p.u.
		8	B1Q12	B1Q3, B1Q1, B1Q10, B1Q31	The other circuit breakers and disconnectors	−1.0 p.u./ −0.3 p.u.
#1 transformer with H line	Outage operation	9	B1Q10	The other circuit breakers and disconnectors	B1Q10, B1Q20, B1Q31, B1Q32, B1Q51, B1Q52	−1.0 p.u./ −0.3 p.u.
		10	B1Q20	The other circuit breakers and disconnectors	B1Q20, B1Q31, B1Q32, B1Q51, B1Q52	−1.0 p.u./ −0.3 p.u.
		11	B1Q31	The other circuit breakers and disconnectors	B1Q31, B1Q32, B1Q51, B1Q52	−1.0 p.u./ −0.3 p.u.
		12	B1Q32	The other circuit breakers and disconnectors	B1Q32, B1Q51, B1Q52	−1.0 p.u./ −0.3 p.u.

trapped charge is −1.0 p.u. (−449 kV) and −0.3 p.u. (−135 kV), respectively.

The points with large VFTO overvoltage amplitude are generally located near the operated switch, 'island' part and electrical terminal etc. We calculate the B phase to ground voltage waveform of some nodes, and select the following nodes for output:

1. Voltage and current of HLA
2. Voltage and current of JLA
3. Voltage and current of #1 LA
4. Voltage and current of #2 LA
5. Voltage of #1 MT
6. Voltage of #2 MMT
7. Voltage of #1 VT
8. Voltage of #2 VT

The changes in amplitude and frequency of VFTO propagating from one end to the other end on long GIS busbar are analyzed. The influence of substation VFTO on the #1 transformer and lightning arresters is evaluated.

3 | RESULTS ANALYSIS AND DISCUSSION

3.1 | Calculation results

Figures 2, 3, 4, 5 and 6 show the VFTO waveform calculated at each measuring point under all of the conditions mentioned above.

The maximum value of VFTO waveform amplitude at each detection point and the maximum value of lightning arrester current are shown in Tables 3 and 4.

When the voltage generated by the trapped charge is −0.3 p.u., the VFTO waveform calculated at each measuring point is similar to that when the voltage generated by the trapped charge is −1.0 p.u., but the amplitude is small. The calculated VFTO

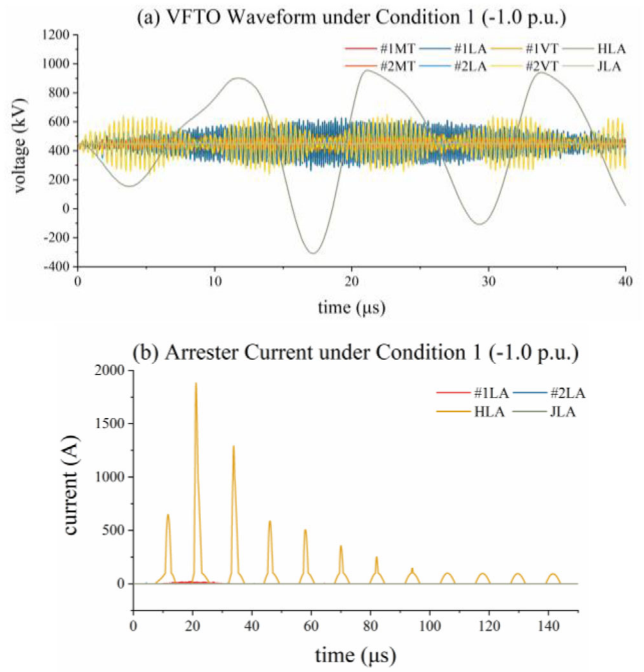

FIGURE 2 When the voltage generated by the trapped charge is −1.0 p.u., (a) showing the voltage at each measuring point calculated under working condition 1, and (b) showing the lightning arrester current

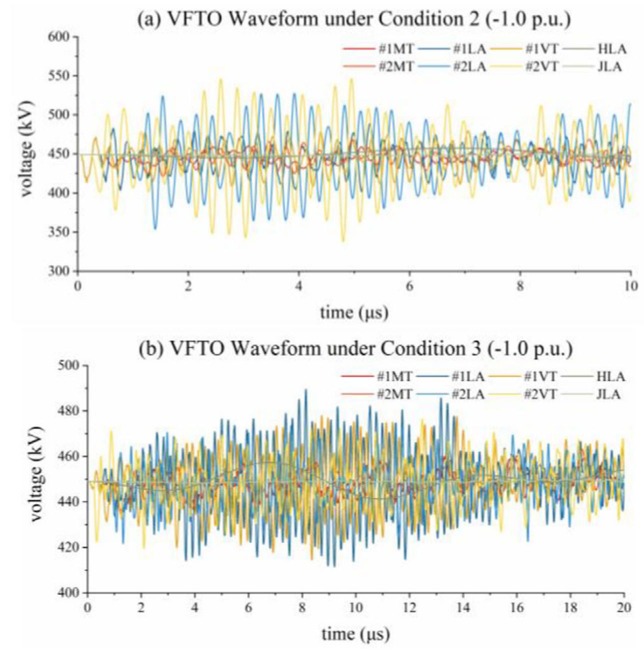

FIGURE 3 When the voltage generated by the trapped charge is −1.0 p.u., (a) showing the voltage at each measuring point calculated under working condition 2, and (b) showing the voltage at each measuring point calculated under working condition 3

waveforms have few high-frequency components, especially at HLA and JLA.

In most calculation conditions, the voltage cannot reach the action voltage of the lightning arrester. When arresters act, the current value of the arrester is not high, and it will act repeatedly in a short time.

3.2 | Maximum value of VFTO voltage waveform

The maximum value of the VFTO voltage waveform at each output node calculated under various working conditions is shown in Table 3.

When the voltage caused by the trapped charge is −1.0 p.u. (−0.3 p.u.), the VFTO voltage waveform amplitudes of #1 MT, #1 LA and #1 VT obtained by disconnecting switch B1Q10 are the largest. The maximum VFTO voltage amplitude obtained at #1 MT is −1132 kV/−2.52 p.u. (−846 kV/−1.88 p.u.), the maximum VFTO amplitude of #1 LA is −1053 kV/−2.35 p.u. (−961 kV/−2.14 p.u.) and the maximum VFTO voltage amplitude of #1 LA node is −898.7 kV/−2.00 p.u. (−872.6 kV/−1.94 p.u.). When the disconnector B1Q20 is operated, the VFTO amplitude at HLA is the largest, and the maximum value is 954.6 kV. The voltage amplitude of the VFTO waveform generated under all simulation conditions at the #1 transformer inlet is less than 1550 kV of impulse withstand voltage of the #1 transformer.

Toda and Ozaki et al. [12] reported that restriking surges caused by DS switching were, at worst, below 2.4 p.u. (1 p.u.: peak value of nominal voltage), which was lower than lightning impulse withstand level (LIWL). They compared the actual measurement results with the EMTP calculation results and found that the actual test results agreed well with the calculation results. Christian and Xie [13] measured the VFTO amplitude at the transformer inlet of an 800-kV hydropower station and found that its peak range is 1.5 to 2.5 p.u. Ma and Li et al. [4] show that the maximum amplitude of VFTO generated in 1100-kV substation is less than 1.5 p.u. We calculated that the VFTO amplitude range of 500-kV substation with long GIS busbar is 1.01 to 2.52 p.u., which is consistent with the maximum amplitude range reported in other literature [5, 18]. Since the stage of reburning is random, the theoretical maximum surge rarely occurs in practical operation. It can be considered that the VFTO amplitude of the 500-kV substation is within the typical value range, and there is no abnormality.

3.3 | Action of lightning arrester

The maximum current of the lightning arrester under various working conditions is shown in Table 4.

The VFTO waveform generated during the I bus outrage operation will not make the arrester act. The VFTO generated in the first step of the H line outrage operation will make the lightning arrester other than JLA act many times and the counter counts frequently. When the voltage amplitude generated by the trapped charge is −1.0 p.u., each step will make #1 LA act during the outrage operation of the main transformer. In the outrage operation of #1 LA with the H line, the first two

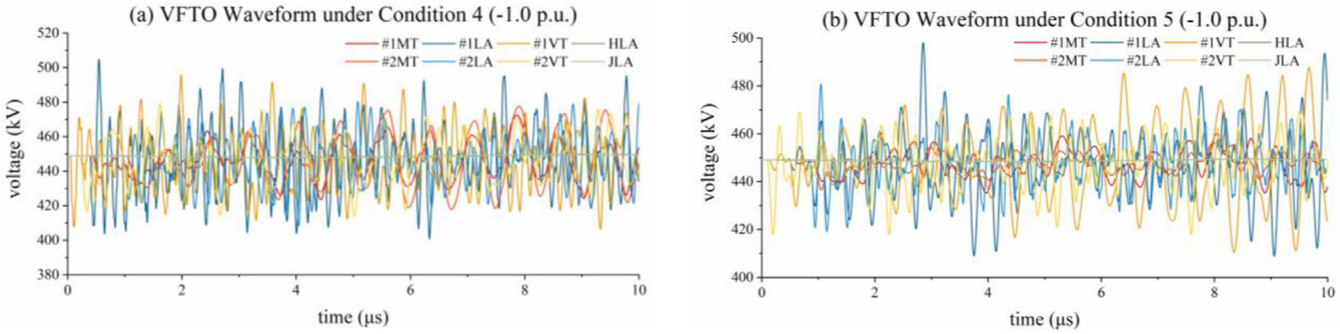

FIGURE 4 When the voltage generated by the trapped charge is −1.0 p.u., (a) showing the voltage at each measuring point calculated under working condition 4, and (b) showing the voltage at each measuring point calculated under working condition 5

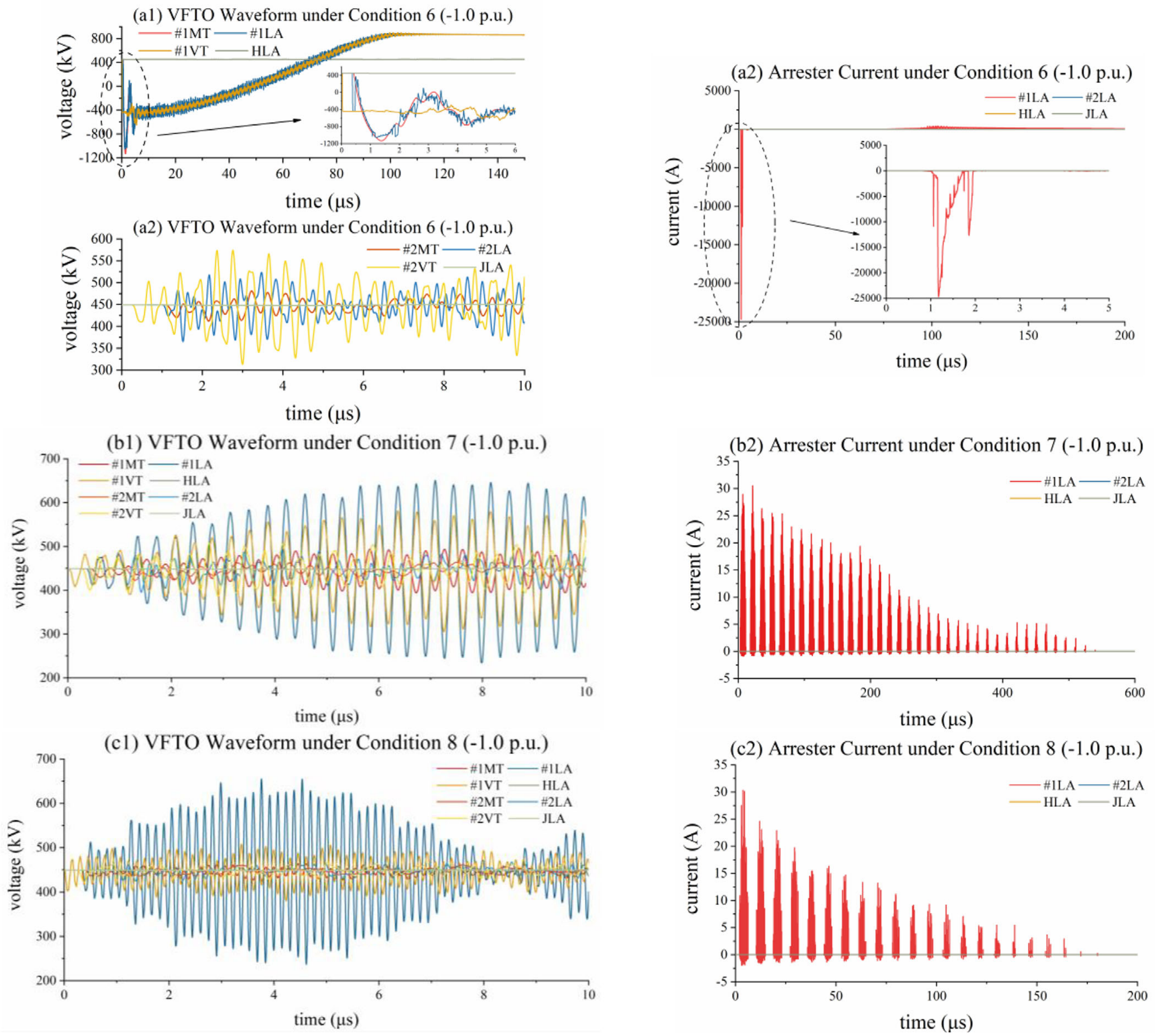

FIGURE 5 When the voltage generated by the trapped charge is −1.0 p.u., (a1) and (a2) showing the voltage at each measuring point calculated under working condition 6, and (a3) showing the lightning arrester current. (b1) Showing the voltage at each measuring point calculated under working condition 7 and (b2) showing the lightning arrester current. (c1) Showing the voltage at each measuring point calculated under working condition 8 and (c2) showing the lightning arrester current under working condition 8

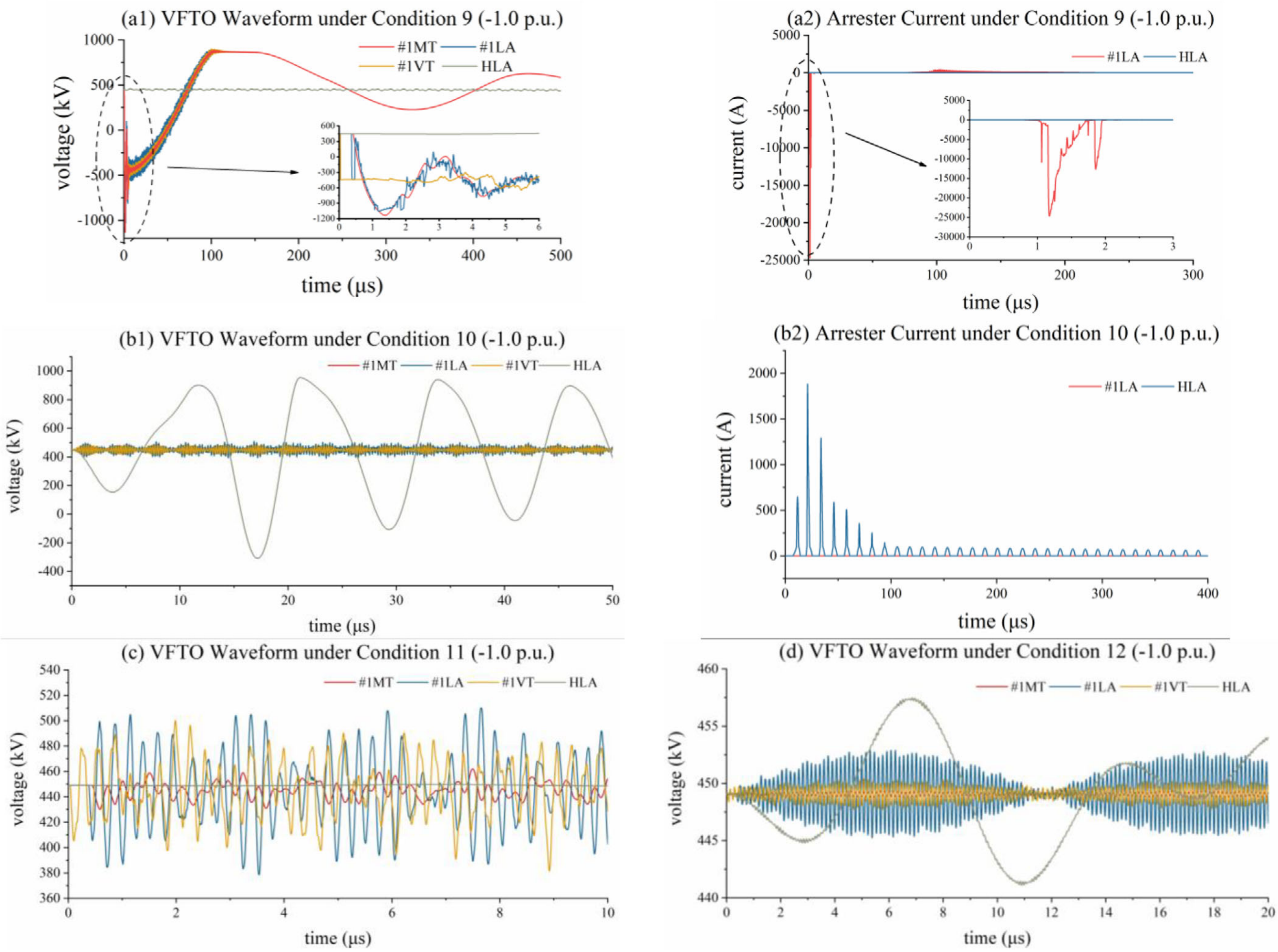

FIGURE 6 When the voltage generated by the trapped charge is −1.0 p.u., (a) shows the voltage at each measuring point calculated under working condition 9, and (b) shows the lightning arrester current. (c) Shows the voltage at each measuring point calculated under working condition 10 and (d) shows the lightning arrester current. (e) Shows the voltage at each measuring point calculated under working condition 11 and (f) shows the voltage at each measuring point calculated under working condition 12

steps make the arrester closest to the operating disconnector act.

When operating the disconnector close to the arrester, such as B1Q10 and B1Q20, the nearest arrester will act. However, when the voltage caused by the trapped charge is −1.0 p.u., the VFTO generated by operating disconnector B1Q20 in condition 1 will make HLA, #1LA and #2 LA act.

3.4 | VFTO voltage waveform frequency analysis

Figure 7 shows the calculation results of the fast Fourier transform of the VFTO waveform obtained in condition 1, condition 4 and condition 6. The VFTO waveform obtained under condition 1 contains more high-frequency components. The amplitude of frequency components greater than 10 MHz cannot be ignored. The amplitude of frequency components exceeding 10 MHz in conditions 4 and 6 is very low. The long GIS bus in the 500-kV substation will reduce the high-frequency component of the VFTO waveform in the system.

Figure 8 shows the S-transform calculation results of the VFTO waveform obtained at #1 MT in conditions 1, 4 and 6. The result of the S-transform is consistent with that of the fast Fourier transform in the main frequency components. From the results of S-transform, the attenuation speed of high-frequency components in VFTO waveform with time is faster, and the attenuation of low-frequency components is slow.

Christian and Xie [13] measured the VFTO at the transformer inlet of an 800-kV hydropower station and found that the total bandwidth of their VFTO results is less than 60 MHz. Ma et al. [14] reported that the dominant oscillating frequencies of the VFTO are 3.5 MHz, 1.6 MHz, and 650 kHz. Haseeb and Thomas [5] using EMTP reported that major frequency components in the simulated VFTO lie in the range of 840 kHz

TABLE 3 Summary of VFTO maximum voltage values under various simulation conditions

Work condition	Operating equipment	Trapped charge	Maximum voltage at #1 MT (kV)	Maximum voltage at #1 LA (kV)	Maximum voltage at #1 VT (kV)	Maximum voltage at #2 MT (kV)	Maximum voltage at #2 LA (kV)	Maximum voltage at #2 VT (kV)	Maximum voltage at H line (kV)	Maximum voltage at J line (kV)
1	B1Q20	−1.0 p.u.	476.9	628.9	524.9	491.8	583.8	651.3	954.6	455.7
		−0.3 p.u.	457.6	503.9	472.2	461.9	489.6	509.9	897.2	450.2
2	B1Q32	−1.0 p.u.	471.8	493	490.9	477.3	551.3	570.5	457.9	455.4
		−0.3 p.u.	462.9	490.2	483.8	463.1	479.3	483.2	457.7	451.2
3	B1Q21	−1.0 p.u.	462.9	490.2	483.8	463.1	479.3	483.2	457.7	451.2
		−0.3 p.u.	454.1	462.5	460.5	454.5	460	461.7	451.6	449.8
4	B1Q11	−1.0 p.u.	447.4	514.9	501.2	487.6	500.4	484.5	450.4	450.4
		−0.3 p.u.	458.1	472.1	467.5	460.7	465.9	460.2	449.5	449.5
5	B2Q11	−1.0 p.u.	478.9	503.9	541.1	461.5	486	485.1	449.9	449.8
		−0.3 p.u.	458.9	467.5	477.6	453.3	463	462.3	449.3	449.3
6	B1Q10	−1.0 p.u.	−1132	−1053	898.7	488.6	533.6	586.2	450.8	451
		−0.3 p.u.	−846	−961	872.6	460.6	474.4	490.2	449.5	449.5
7	B1Q31	−1.0 p.u.	500.1	655.5	584.4	483.7	516.7	535.3	450.9	451
		−0.3 p.u.	465.1	513.8	492.7	459.9	470.9	475.9	449.6	449.7
8	B1Q12	−1.0 p.u.	470.5	654.9	508.1	467.8	473.7	472.8	450.3	450.3
		−0.3 p.u.	454.9	512	466.9	456	458.5	458.2	449.5	449.5
9	B1Q10	−1.0 p.u.	−1132	−1053	898.7	-	-	-	457.9	-
		−0.3 p.u.	−846	−961	872.6	-	-	-	451.7	-
10	B1Q20	−1.0 p.u.	454.5	508.7	487.3	-	-	-	954.6	-
		−0.3 p.u.	450.7	467	460.6	-	-	-	897.2	-
11	B1Q31	−1.0 p.u.	466.9	521.1	504.4	-	-	-	449.7	-
		−0.3 p.u.	454.3	470.5	465.6	-	-	-	449.2	-
12	B1Q32	−1.0 p.u.	449.4	452.9	450.4	-	-	-	449.2	-
		−0.3 p.u.	449.2	450.2	449.5	-	-	-	451.6	-

*'-' means that the influence of VFTO on the fundamental wave can be ignored.

to 30 MHz. Povh and Schmitt et al. [17] figured that the main frequencies of the VFT depend on the length of the GIS section affected by the disconnector switch operation and are in the range of 1 MHz up to 40 MHz for the basic component. Ma and Li et al. [4] indicate that the main frequency components of the typical VFTO waveform are 0.69, 1.43, 1.83, 2.27 and 6.83 MHz. They found that since the busbar of the UHV substation is significantly longer than that of the test base, the main frequency measured in the substation is lower than that of the test base, and the high-frequency components are reduced by the larger capacitance of the busbar, while the lower frequency components last longer due to the longer transmission distance. The VFTO frequency range of 500-kV substation with long GIS busbar calculated by us is 10 kHz to 50 MHz, and the main frequencies of most simulation conditions are 0.02, 0.34, 1.8 and 6.5 MHz. Due to the existence of long GIS busbar, the content of the low-frequency component in the VFTO waveform is high, and the high-frequency component has been significantly attenuated when it propagates to the entrance of the transformer.

3.5 | Discussion

There is a long GIS busbar between the #1 VT node and #1 LA node and between #2 VT and #2 LA. When the operating disconnectors close to #1 VT, #1 LA and #1 MT (such as B1Q10, B1Q32 and B1Q11) are operated, the magnitude of VFTO voltage of #2 VT is greater than #2 LA, but the magnitude of VFTO voltage of #1 VT is less than #1 LA. When the disconnectors close to #2 VT, #2 LA and #2 MT (such as B2Q11) are operated, the magnitude of VFTO voltage is the opposite. Li and Shang et al. [11] reported that the maximum amplitude obtained by field measurement is 2.19 p.u. and VFTO magnitudes on the source sides of the disconnectors are generally smaller than those on the load sides. The magnitude range for the load sides is from 1.92 to 2.46 p.u. While for the source sides the range is larger from 1.06 and 2.26 p.u. When the length of energized GIS duct on the source side is long, the oscillations and VFTO magnitudes are large. When the length on the source side is quite short, the oscillations and VFTO magnitudes are small. Contrary to their results, when operating the disconnector

TABLE 4 Summary of maximum current of lightning arrester

Work Condition	Operating equipment	Trapped charge	Maximum current at #1 LA (A)	Maximum current at #2 LA (A)	Maximum current at HLA (A)	Maximum current at JLA (A)
1	B1Q20	−1.0 p.u.	21.54	6.33	1882.09	-
		−0.3 p.u.	-	-	596.47	-
2	B1Q32	−1.0 p.u.	-	-	-	-
		−0.3 p.u.	-	-	-	-
3	B1Q21	−1.0 p.u.	-	-	-	-
		−0.3 p.u.	-	-	-	-
4	B1Q11	−1.0 p.u.	-	-	-	-
		−0.3 p.u.	-	-	-	-
5	B2Q11	−1.0 p.u.	-	-	-	-
		−0.3 p.u.	-	-	-	-
6	B1Q10	−1.0 p.u.	−24684.59	-	-	-
		−0.3 p.u.	−1990.39	-	-	-
7	B1Q31	−1.0 p.u.	30.51	-	-	-
		−0.3 p.u.	-	-	-	-
8	B1Q12	−1.0 p.u.	30.34	-	-	-
		−0.3 p.u.	-	-	-	-
9	B1Q10	−1.0 p.u.	−24684.59	-	-	-
		−0.3 p.u.	−1990.39	-	-	-
10	B1Q20	−1.0 p.u.	-	-	1882.09	-
		−0.3 p.u.	-	-	596.47	-
11	B1Q31	−1.0 p.u.	-	-	-	-
		−0.3 p.u.	-	-	-	-
12	B1Q32	−1.0 p.u.	-	-	-	-
		−0.3 p.u.	-	-	-	-

* '-' means that the current of the arrester is less than 1 mA, and the arrester does not act.

close to the outgoing line, the calculated VFTO voltage amplitude that may occur is less than the VFTO voltage amplitude that may occur when operating the disconnector close to the power supply. Under some working conditions, the VFTO voltage amplitude of # 1VT calculated by us is less than that of # 1 LA. This shows that when the VFTO waveform passes through a long GIS bus, the amplitude may become larger.

Christian and Xie [13] measured the VFTO amplitude at the transformer inlet of an 800-kV hydropower station and found that its peak range is 1.5 to 2.5 p.u. The total bandwidth of their VFTO results is less than 60 MHz. Such values are well known and typical for large GIS substations. Filho et al. [21] introduced that when the VFTO amplitude is lower than the basic pulse level, the cumulative effect of a series of peak voltages will lead to the failure of the power transformer. It was found that the time to voltage peak, the inner frequency bandwidth and the voltage peak values around 2.0 to 2.8 times the nominal voltage [22] lay within the ranges suggested in IEC 60071-1 [23]. The maximum VFTO voltage calculated by us does not exceed the impulse withstand voltage of the #1 transformer. The two outgoing lines of the 500-kV GIS step-up substation frequently trip after being put into operation. The #1 transformer, #1 voltage transformer and #1 lightning arrester of 500-kV GIS step-up substation were damaged after the B phase grounding short circuit fault of Line H and Line J. Before the fault, there was no obvious abnormality in the operation of the equipment in the substation. Considering that the fault current at the last fault did not exceed the range that the #1 transformer can bear. Therefore, for substations with frequently operated switchgear, although the maximum amplitude of #1MT VFTO calculated in this paper is less than its impulse withstand voltage, due to too many outgoing line faults and frequent action of disconnectors, it is necessary to consider the cumulative effect and pay more attention to the operating conditions of voltage transformers, lightning arresters and transformers.

In actual operation, a more efficient maintenance plan should be set for equipment prone to damage according to the simulation results, so as to find potential faults and improve the operation stability of the power system. However, how many times the transformer insulation will be damaged after withstanding the impact is a problem that needs further observation and research in the future.

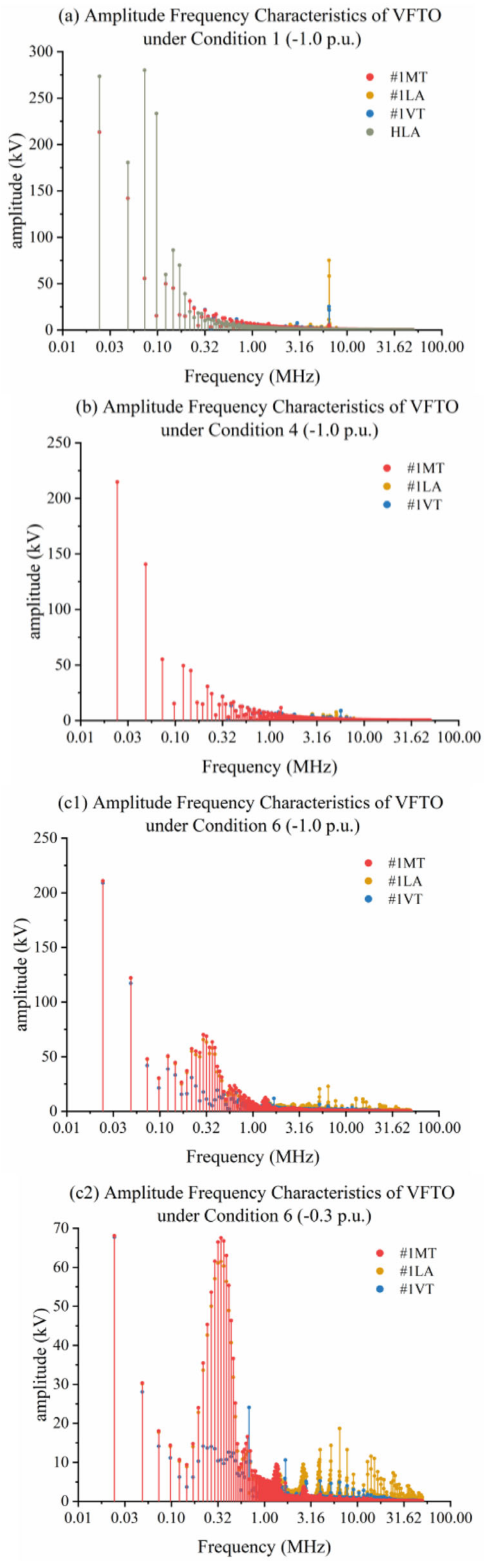

FIGURE 7 When the voltage generated by the trapped charge is −1.0 p.u., (a) showing the amplitude frequency characteristics of VFTO obtained under condition 1, and (b) showing the amplitude frequency characteristics of VFTO obtained under condition 4. (c1) Showing the amplitude frequency characteristics of VFTO obtained under condition 6, when the voltage generated by the trapped charge is −1.0 p.u. (c2) Showing the amplitude frequency characteristics of VFTO obtained under condition 6, when the voltage generated by the trapped charge is −0.3 p.u.

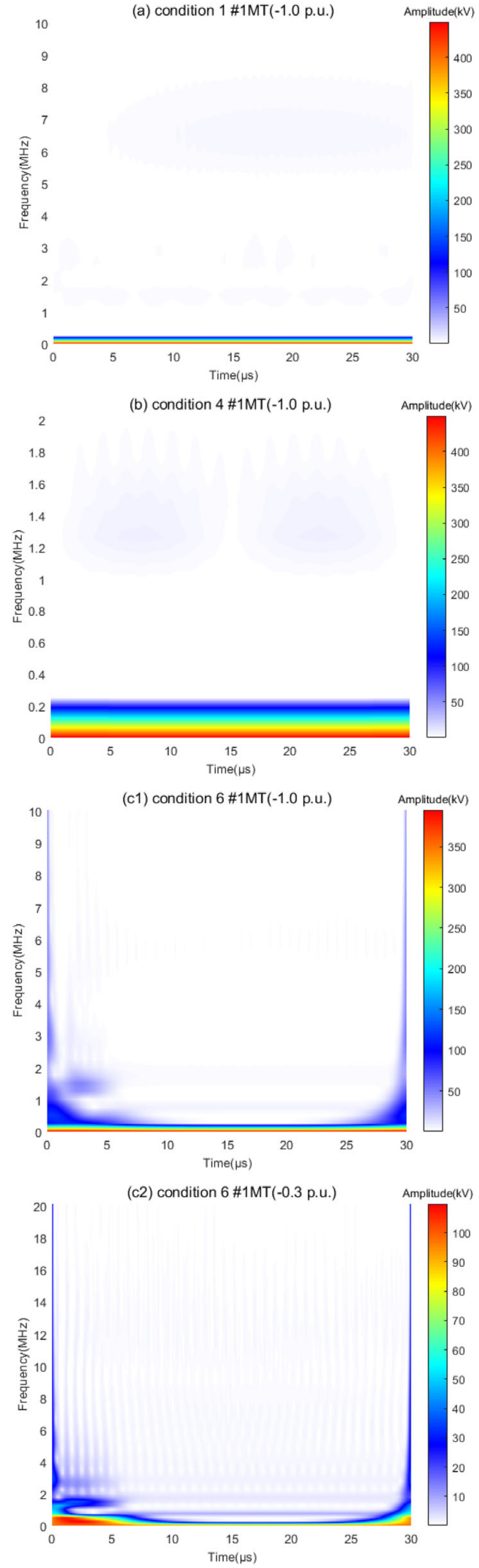

FIGURE 8 When the voltage generated by the trapped charge is −1.0 p.u., (a) showing the S-transformation calculation results of VFTO obtained under condition 1, and (b) showing the S-transformation calculation results of VFTO obtained under condition 4. (c1) Showing the S-transformation calculation results of VFTO obtained under condition 6, when the voltage generated by the trapped charge is −1.0 p.u. (c2) Showing the S-transformation calculation results of VFTO obtained under condition 6, when the voltage generated by the trapped charge is −0.3 p.u.

4 | CONCLUSION

In this paper, we use EMTP simulation software to simulate the VFTO waveform that may be generated in different operation steps of a 500-kV power plant step-up substation. We analyze the amplitude and frequency of the obtained VFTO waveform and observe the action of the arrester. The main conclusions are as follows.

When operating the disconnector close to the transformer, the VFTO waveform amplitude may be as high as 1000 kV at the #1 MT node. The maximum value of VFTO amplitude obtained at the #1 MT node is −1132 kV, which is less than 1550 kV of impulse withstand voltage of the transformer. After the VFTO waveform generated by operating the disconnector near 1 VT propagates through the GIS busbar between 1 VT and 1 LA, the amplitude of VFTO will increase.

The VFTO waveform generated when operating the disconnector close to the arrester will cause the action of the arrester. Due to the high frequency of the VFTO waveform, the arrester will act many times and count frequently in a short time. Under some conditions, the operation of the disconnector will also make the remote arrester act and count.

In this 500-kV substation with long GIS busbar and double circuit, the low-frequency component accounts for a large proportion of VFTO waveform. The attenuation rate of the high-frequency component in the VFTO waveform with time is faster than that of the low-frequency component, and the low-frequency component hardly attenuates within 30 μs.

AUTHOR CONTRIBUTIONS

Runyu Fu: Investigation, Data Curation, Formal analysis, Visualization, Writing-Original Draft. Jianguo Wang: Conceptualization, Methodology, Writing - Review & Editing, Project administration. Jianping Wang: Supervision, Validation, Writing-Original Draft. Mi Zhou: Resources, Investigation. Li Cai: Resources, Supervision. Yating Zhao: Validation, Investigation. Yadong Fan: Validation, Supervision.

CONFLICT OF INTEREST

The authors declare no competing interests.

FUNDING INFORMATION

This article has no fund support.

DATA AVAILABILITY STATEMENT

No data available in this article

ORCID

Runyu Fu https://orcid.org/0000-0002-0479-7606
Yating Zhao https://orcid.org/0000-0001-5462-5231

REFERENCES

1. Boggs, S.A., Chu, F.Y., Fujimoto, N., et al.: Disconnect switch induced transients and trapped charge in gas-insulated substations. IEEE Trans. Power Appar. Syst. PAS-101(10), 3593–3602 (1982)
2. Meppelink, J., Diederich, K.J., Feser, K., et al.: Very fast transients in GIS. IEEE Trans. Power Deliver. 4(1), 223–233 (1989)
3. Zhang, L., Zhang, Q., Liu, S., et al.: Insulation characteristics of 1100 kV GIS under very fast transient overvoltage and lightning impulse. IEEE Trans. Dielectr. Electr. Insul. 19(3), 1029–1036 (2012)
4. Ma, G.-.M., Li, C.-.R., Li, X., et al.: Time and frequency characteristics of very fast transient overvoltage in ultra high voltage substation. IEEE Trans. Dielectr. Electr. Insul. 24(4), 2459–2468 (2017)
5. Haseeb, M.A., Thomas, M.J.: Computation of very fast transient overvoltages (VFTO) in a 1000 kV gas insulated substation. In: Proceedings of 2017 IEEE PES Asia-Pacific Power and Energy Engineering Conference (APPEEC), pp. 1–6 (2017)
6. Bian, H., Cao, M., Kai, Z., et al.: Filtering for the interference signal caused by grounding potential difference in high-voltage disconnector. IEEE Sens. J. 21(6), 7768–7775 (2021)
7. Gong, W., Wang, P., Li, Q., et al.: Simulation of VFTO suppression methods for 1100 kV GIS substation. In: Proceedings of the 2019 IEEE 3rd Information Technology, Networking, Electronic and Automation Control Conference (ITNEC), pp. 987–991 (2019)
8. Lu, B., Shi, Y., Zhan, H., et al.: VFTO suppression by selection of a combination of initial phase angle and contact velocity. IEEE Trans. Power Deliver. 33(3), 1115–1123 (2018)
9. Lu, B., Shi, Y., Lin, X., et al.: 3d full Maxwell research for effect of initial electromagnetic field on very fast transient overvoltage in GIS. IEEE Trans. Dielectr. Electr. Insul. 23(6), 3319–3327 (2016)
10. Szewczyk, M., Kutorasiński, K., Wroński, M., et al.: Full-Maxwell simulations of very fast transients in GIS: Case study to compare 3-d and 2-d-axisymmetric models of 1100 kV test setup. IEEE Trans. Power Deliver. 32(2), 733–739 (2017)
11. Li, Y., Shang, Y., Zhang, L., et al.: Analysis of very fast transient overvoltages (VFTO) from onsite measurements on 800 kV GIS. IEEE Trans. Dielectr. Electr. Insul. 19(6), 2102–2110 (2012)
12. Toda, H., Ozaki, Y., Miwa, I., et al.: Development of 800 kV gas-insulated switchgear. IEEE Trans. Power Deliver. 7(1), 316–323 (1992)
13. Christian, J., Xie, J.: Very fast transient oscillation measurement at three gorges left bank hydro power plant. In: Proceedings of the 2006 International Conference on Power System Technology, pp. 1–7 (2006)
14. Ma, G.-.M., Li, C.-.R., Quan, J.-.T., et al.: Measurement of VFTO based on the transformer bushing sensor. IEEE Trans. Power Deliver. 26(2), 684–692 (2011)
15. Shu, Y., Chen, W., Li, Z., et al.: Experimental research on very-fast transient overvoltage in 1100-kV gas-insulated switchgear. IEEE Trans. Power Deliver. 28(1), 458–466 (2013)
16. Cheng, L., Lei, L., Ruan, X., et al.: Analysis of VFTO signal characteristics under the operation of isolating switch in GIS. In: Proceedings of 2020 6th Global Electromagnetic Compatibility Conference (GEMCCON), pp. 1–4. (2020)
17. Povh, D., Schmitt, H., Valcker, O., et al.: Modelling and analysis guidelines for very fast transients. IEEE Trans. Power Deliver. 11(4), 2028–2035 (1996)
18. Seo, H., Jang, W., Kim, C., et al.: Analysis of magnitude and rate-of-rise of VFTO in 550 kV GIS using EMTP-RV. J. Electr. Eng. Technol. 8(1), 11–19 (2013)
19. Narimatsu, S., Yamaguchi, K., Nakano, S., et al.: Interrupting performance of capacitive current by disconnecting switch for gas insulated switchgear. IEEE Power Eng. Rev. PER-1(6), 36–37 (1981)
20. Zhang, Q., Jia, J., Yang, L., et al.: Mechanism of discharge development in SF6 with and without spacers under fast oscillating impulse condition. J Appl. Phys. 98(10), 103301 (2005)
21. Guilherme Rodrigues Filho, J., Arinos Teixeira, J., Rot Sans, M., et al.: Very fast transient overvoltage waveshapes in a 500-kV gas insulated switchgear setup. IEEE Electr. Insul. Mag. 32(3), 17–23 (2016)

22. Insulation co-ordination. Computational guide to insulation co-ordination and modelling of electrical networks. *Book* Insulation co-ordination. Computational guide to insulation co-ordination and modelling of electrical networks, Series Insulation co-ordination. Computational guide to insulation co-ordination and modelling of electrical networks, IEC TR 60071–4 ed., Editor ed., pp. 13.
23. Insulation co-ordination – part 1: definitions, principles and rules (IEC 60071-1:2006). *Book* Insulation co-ordination – part 1: definitions, principles and rules (IEC 60071-1:2006), Series Insulation co-ordination – part 1: definitions, principles and rules (IEC 60071-1:2006), IEC 60071-1 ed., Editor ed., pp. 33.

How to cite this article: Fu, R., Wang, J., Wang, J., Zhou, M., Li, C., Zhao, Y., Fan, Y.: Very fast transient overvoltage calculation and evaluation for 500-kV gas insulated substation power substation with double circuit and long gas insulated substation busbar. IET Gener. Transm. Distrib. 17, 252–262 (2023). https://doi.org/10.1049/gtd2.12680